

See discussions, stats, and author profiles for this publication at: <http://www.researchgate.net/publication/275965257>

Using high-resolution numerical weather forecasts to improve remotely sensed rainfall estimates: The case of the 2013 Colorado flash flood.

ARTICLE in JOURNAL OF HYDROMETEOROLOGY · APRIL 2015

Impact Factor: 3.65 · DOI: 10.1175/JHM-D-14-0207.1

READS

37

4 AUTHORS:



Efthymios I. Nikolopoulos

University of Padova

59 PUBLICATIONS 199 CITATIONS

SEE PROFILE



Nikolaos Bartsotas

National and Kapodistrian University of ...

11 PUBLICATIONS 1 CITATION

SEE PROFILE



Emmanouil N. Anagnostou

University of Connecticut

253 PUBLICATIONS 2,262 CITATIONS

SEE PROFILE



George Kallos

National and Kapodistrian University of ...

226 PUBLICATIONS 3,129 CITATIONS

SEE PROFILE

Using High-Resolution Numerical Weather Forecasts to Improve Remotely Sensed Rainfall Estimates: The Case of the 2013 Colorado Flash Flood

E. I. NIKOLOPOULOS

Innovative Technologies Center S.A., Athens, Greece

N. S. BARTSOTAS

Department of Physics, University of Athens, Athens, Greece

E. N. ANAGNOSTOU

Department of Civil and Environmental Engineering, University of Connecticut, Storrs, Connecticut

G. KALLOS

Department of Physics, University of Athens, Athens, Greece

(Manuscript received 20 October 2014, in final form 4 March 2015)

ABSTRACT

The September 2013 flash flood-triggering rainfall event in Colorado highlighted the strong underestimation of remote sensing techniques over mountainous terrain. In this work, the use of high-resolution rainfall forecasts for adjusting weather radar- [Multi-Radar Multi-Sensor (MRMS) quantitative precipitation estimation (Q3)] and satellite-based [CPC morphing technique (CMORPH) and TRMM 3B42RT] rainfall estimates is examined. Evaluation of the adjustment procedures is based on the NCEP Stage IV product. Results show that 1-km-grid-resolution rainfall forecasts provided by a numerical weather prediction model [Regional Atmospheric Modeling System and Integrated Community Limited Area Modeling System (RAMS-ICLAMS)] adequately captured total rainfall amounts during the event and could therefore be used to adjust biases in radar and satellite rainfall estimates. Two commonly used adjustment procedures according to 1) mean field bias and 2) probability density function matching are examined. Findings indicate that both procedures are successful in improving the original radar and satellite rainfall estimates, with the first method consistently providing the highest bias reduction while the second exhibits higher improvement in RMSE and correlation.

1. Introduction

Starting on 9 September 2013, a stationary low pressure system centered west of Colorado, resulting in high (>200 mm) rain accumulations that caused catastrophic flash floods along Colorado's Front Range from Colorado Springs north to Fort Collins. According to U.S. Federal Emergency Management Agency reports, the flooding killed 10 people and destroyed 1882 structures, damaging at least 16 000 others.

The September 2013 Colorado flood event highlighted a strong underestimation of quantitative precipitation estimation (QPE) from remote sensing observations (Gochis et al. 2015). Underestimation of heavy precipitation was long ago recognized for radar-based techniques (e.g., Wilson and Pollock 1974; Smith et al. 1996) and more recently for satellite-based techniques (Habib et al. 2009; Nikolopoulos et al. 2013; Stampoulis et al. 2013). Improving remote sensing QPE is a rather old but still open topic of research. In radar-based QPE, numerous studies have focused on the development and application of mean field and range effect correction procedures (e.g., Krajewski 1987; Seo and Breidenbach 2002; Chumchean et al. 2006; Goudenhoofd and Delobbe 2009; Wang et al. 2012), while over the last decade, bias correction procedures have been developed for satellite-based QPE (Yin et al. 2008;

Corresponding author address: Efthymios I. Nikolopoulos, Department of Land, Environment, Agriculture and Forestry, University of Padua, Campus di Agripolis, Viale dell'Università 16, 35020 Legnaro PD, Italy.
E-mail: efthymios.nikolopoulos@unipd.it

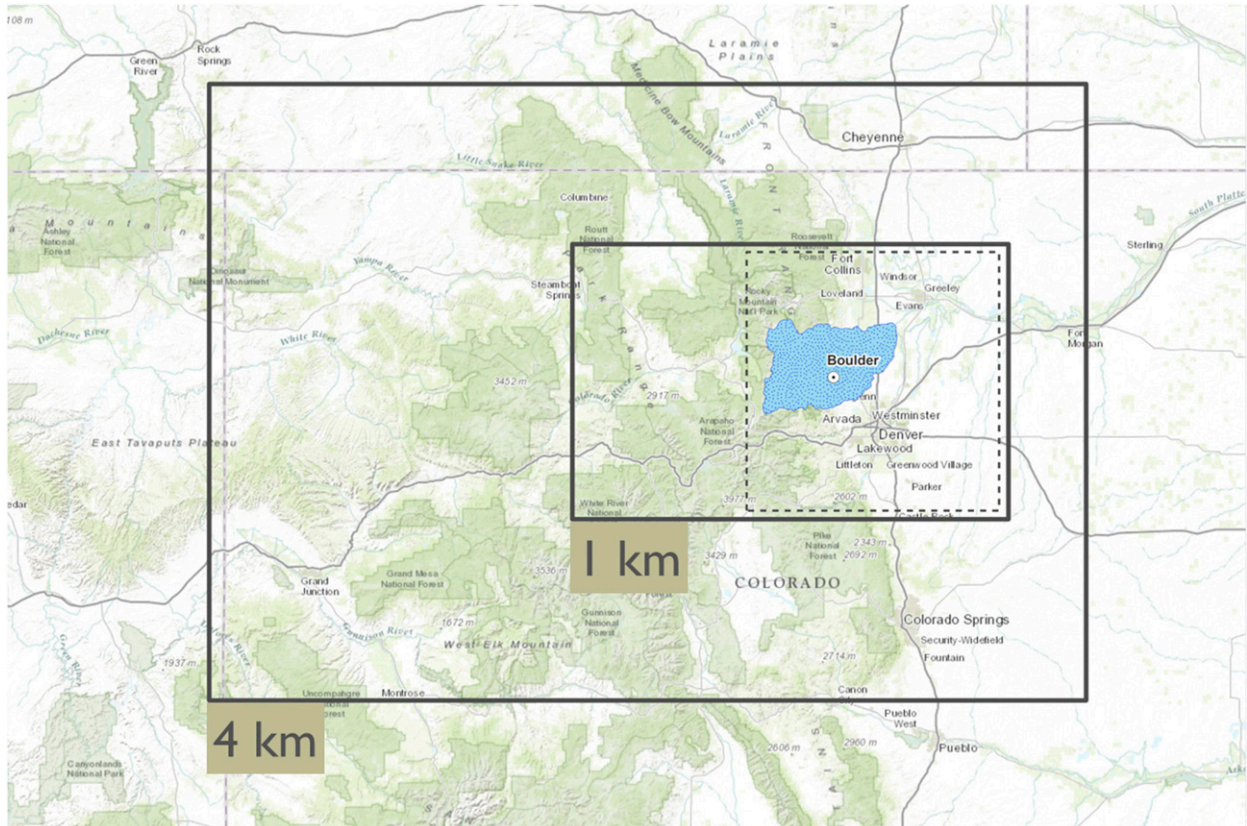


FIG. 1. Map showing the extent of the RAMS-ICLAMS domain at 4- and 1-km pixel resolutions and the area of analysis (dashed rectangle). The blue shaded area within the analysis domain corresponds to areal coverage of St. Vrain basin.

Boushaki et al. 2009; Tesfagiorgis et al. 2011; Müller and Thompson 2013). Results from these works have demonstrated improvements in QPE, but their common characteristic is that they are conditional to availability of in situ observations. This condition limits their applicability over areas with sparse or nonexistent ground observations, such as mountainous areas, which are particularly prone to flash flooding. An alternative solution to this limitation may be the use of high-resolution numerical weather prediction (NWP) model simulations, as shown in the recent work by Zhang et al. (2013), who demonstrated that such an approach improved satellite QPE during heavy precipitation events in a western Mediterranean mountainous area.

Following the general methodological framework of Zhang et al. (2013), the objective of this work is to investigate and demonstrate how the use of high-resolution NWP forecasts could have improved radar and satellite QPE for the 2013 Colorado flash flood event. This work expands on that of Zhang et al. (2013) in two main aspects. First, a different NWP model is applied at high (1 km) resolution and simulated rainfall is based on forecasted fields, while Zhang et al. (2013) used Weather Research

and Forecasting Model simulations at 2-km resolution based on reanalysis data. Investigating the effectiveness of this approach based on forecasted precipitation allows us to evaluate its potential in real-time QPE. Second, Zhang et al. (2013) examined the application of the technique on CPC morphing technique (CMORPH) satellite estimates, while in this work we examine two additional real-time precipitation products coming from a global-scale satellite product [Tropical Rainfall Measuring Mission (TRMM) 3B42RT] and the National Weather Service Multi-Radar Multi-Sensor (MRMS) system, which allows us to examine the efficiency of the proposed methodology for precipitation products with different characteristics (resolution, retrieval algorithm, etc.).

2. Study area and data

a. Area of analysis

The overall domain of analysis in this study covers an area of $\sim 1.5^\circ \times 1.5^\circ$ centered on Boulder, Colorado (Fig. 1), thus focusing on the region that was mainly impacted by the heavy precipitation event. Topography

TABLE 1. Spatiotemporal resolution and timeliness of the precipitation products used.

Product	Spatial resolution (km)	Temporal resolution (h)	Availability with respect to real time	Source of description
Stage IV	4	1	1–12 h after	www.emc.ncep.noaa.gov/mmb/ylin/pcpanl/Qanda/#ST4TIME
RAMS-ICLAMS	1	1	24 h before	*
MRMS/Q3	1	1	2–3 min after	Zhang et al. (2011)
3B42RT	~25	3	~7 h after	ftp://trmmopen.gsfc.nasa.gov/pub/merged/V7Documents/3B4XRT_doc_V7.pdf
CMORPH	~8	0.5	~18 h after	www.cpc.ncep.noaa.gov/products/janowiak/cmorph_description.html

* Number corresponds to the specific setup used. Note that the forecast lead time can vary considerably according to the available computational power and procedure (e.g., size of forecasting window) used.

of the region is highly complex, with elevations ranging from 1300 to 4350 m MSL and averaging 2100 m MSL. Analysis is further concentrated on the St. Vrain basin, which covers approximately 2700 km² (Fig. 1) and includes many areas where severe flooding occurred during the event under study.

b. Remotely sensed rainfall products

Four remotely sensed rainfall products, available at different spatiotemporal resolutions (see Table 1) are utilized in this work. The first is the National Centers for Environmental Prediction (NCEP) Stage IV precipitation product (Lin and Mitchell 2005), which is a derivative of radar and gauge analysis, available approximately 1–12 h past real time. QPEs for this product are based on the radar-rainfall estimates obtained from the standard National Weather Service precipitation algorithm (Fulton et al. 1998) after bias adjustment from rain gauges at the hourly scale. The second product is the MRMS quantitative precipitation estimation (MRMS/Q3; hereafter denoted as Q3), which is the QPE product of the MRMS that is based only on the real-time radar-rainfall fields (i.e., no gauge adjustment involved) and is available 2–3 min past real time. In this product, radar echoes are classified to the different precipitation type (stratiform, convective, tropical, etc.) and a specific reflectivity–rainfall relationship (commonly known as a Z – R relationship) is used for each class (Zhang et al. 2011). The third product involved is the 3B42RT, which is the near-real-time (~7 h past real time) version of TRMM Multisatellite Precipitation Analysis (TMPA) from the National Aeronautics and Space Administration (NASA). Rainfall estimates in this product are derived as a combination of infrared- and microwave-based satellite observations (Huffman et al. 2007). Note that in this work we have used the calibrated version of 3B42RT, version 7 (3B42RTv7), which is the original real-time product adjusted according to a climatological bias correction derived from 3B42, version 6. The fourth and last product involved is CMORPH from the National

Oceanic and Atmospheric Administration (NOAA). Rainfall estimates from CMORPH are available about 18 h past real time and are obtained exclusively from satellite-based microwave observations that are propagated spatiotemporally by infrared-derived motion vector images (Joyce et al. 2004).

c. Forecasted rainfall

The atmospheric simulations were produced by the Regional Atmospheric Modeling System and Integrated Community Limited Area Modeling System, version 1.3 (RAMS-ICLAMS; Solomos et al. 2011; Kushta et al. 2014), with a setup of three nested grids. The horizontal grid spacing of the coarse grid was set to 24 km (125 × 84 points), and it stretched in the longitudinal axis from 130.8° to 88.2°W and in the latitudinal axis from 27.3° to 53.9°N. The extents of the intermediate domain of 4 km (122 × 86 points) as well as the inner domain of 1 km (242 × 162 points) are illustrated in Fig. 1. Time steps were set to 30, 5, and 1.25 s for the 24-, 4-, and 1-km grids, respectively, while all three domains featured 32 vertical levels.

Initial and boundary conditions were provided by NCEP GFS analyses and forecasts, respectively. The model includes an advanced microphysical scheme (Meyers et al. 1997) with eight categories of water (vapor, cloud droplets, rain droplets, pristine ice, snow, aggregates, graupel, and hail) and an interactive mineral dust and sea salt cycle. The radiative transfer scheme in the model [Rapid Radiative Transfer Model (RRTM); Mlawer et al. 1997; Iacono et al. 2000] includes the aerosol feedbacks on radiation fluxes. Activation of cloud condensation nuclei into cloud droplets is explicitly computed with the scheme of Fountoukis and Nenes (2005) based on the properties of airborne particles. The formation of ice nuclei is also calculated online with the scheme of Barahona and Nenes (2009) based on the modeled air quality properties. Topographic representation was based on high-resolution (90 m at the equator) terrain elevation data provided by the NASA Shuttle Radar Topography Mission (SRTM)

90 (Farr et al. 2007) topography. The final forecasted rainfall fields used in the analysis emerged as a synthesis of retrospective simulations that represent the operational daily forecasting procedure. This involved initialization of the model with the GFS 1200 UTC cycle and the generation of forecasts with a forecasting window of 36 h, from which the first 12 h served as spinoff period and the remaining 24 h comprised the forecasted rainfall data of the next day. The process was repeated with the GFS forecast of the next day, until the last day of the event considered.

3. Methodology

The Stage IV rainfall product is used throughout the analysis as the “ground truth” reference. Therefore, all the error metrics used for the evaluation of original and adjusted versions of products Q3, CMORPH, and 3B42RT [called collectively rainfall products under evaluation (RPUE)] are calculated with reference to the Stage IV product. However, adjustment of the RPUE is based on the forecasted rainfall fields (RAMS-ICLAMS) used as reference. An important note here is that, because of the differences in spatial and temporal resolution of products under study, adjustment and comparison procedures are carried out at different space–time scales for each RPUE. Consequently, reference and RPUE were aggregated to a common space–time resolution (4 km and 1 h for Q3, $\sim 0.07^\circ$ and 1 h for CMORPH, and 0.25° and 3 h for 3B42RT).

Adjustment of the RPUE is carried out following two basic methods. The first is the mean field bias (MFB) adjustment, which involves the calculation of a single adjustment factor derived as the ratio of the spatially averaged (over the analysis domain) accumulated rainfall values between RPUE and the NWP reference product (i.e., RAMS-ICLAMS). Essentially, the method derives a constant adjustment factor, which is used to scale the original RPUE estimates. In addition to the advantage of simplicity of this method, the adjusted RPUE preserves the reference mean field accumulated rainfall. However, a potential shortfall of this method is its inability to capture the potential bias dependence on rainfall magnitude.

The second method is the probability density function (PDF) matching procedure that allows accounting for the rainfall magnitude dependence of bias. As in Zhang et al. (2013), PDF matching procedure adjusts individual quantiles of RPUE distribution to the corresponding reference quantiles. Note that PDFs are calculated considering all rainfall values over the spatial and temporal analysis domain, obtained at the common spatiotemporal scale of reference and RPUE at each case (as previously mentioned).

Evaluation of the original and adjusted RPUE is carried out on both spatial and temporal domain.

Comparison in space is performed by contrasting the reference (Stage IV) with RPUE accumulated rainfall fields (over the whole domain of the analysis) and aims to evaluate the differences in the spatial representation of the overall rainfall pattern. Analysis in the temporal domain is carried out by comparing the reference and RPUE basin-averaged rainfall time series and aims to assess differences in the representation of rainfall temporal dynamics. Three common statistical metrics are used for the comparison, namely, the bias ratio representing the ratio of reference rainfall to the total RPUE (or forecasted) rainfall, root-mean-square error (RMSE), and correlation coefficient.

4. Results and discussion

This section summarizes the results from the comparison of original and adjusted RPUE with reference rainfall. The rainfall period analyzed spans from 0000 UTC 9 September to 2300 UTC 13 September 2013.

a. Comparison of observed and simulated rainfall

Accumulated rainfall fields from all original datasets (Stage IV, MRMS/Q3, CMORPH, and 3B42RT) are presented in Fig. 2 and the corresponding total rainfall amounts averaged over the entire analysis domain and the basin are reported in Table 2. The first striking feature from these results is the strong underestimation of all RPUEs, which represent only 30%–50% of the reference rainfall (Stage IV). Underestimation is consistent and approximately equal in both scales (basin and entire domain).

Accumulated rainfall from RAMS-ICLAMS captures the domain-averaged rainfall accumulation but underestimates total rainfall over the basin by $\sim 15\%$. This suggests that the MFB adjustment technique will result in RPUE estimates with correct domain-averaged total rainfall amounts. However, discrepancies in total rainfall at smaller scales (e.g., over the basin) are expected given the spatial variability of bias over the domain. Overall, the RAMS-ICLAMS accumulated rainfall patterns represent the rainfall distribution over the western part of the domain well, while on the eastern part rainfall appears somewhat misplaced and a high rainfall band in the center of the domain (shown in Stage IV map) does not appear in the RAMS-ICLAMS map.

The overall distribution of rainfall between RPUE and reference (Stage IV or RAMS-ICLAMS) products is compared using quantile–quantile (Q – Q) plots (Fig. 3). For each case/product, rainfall distribution is derived from rainfall estimates at the specified common space–time scale (see section 3). The Q – Q plots show that underestimation of RPUE is consistent over the

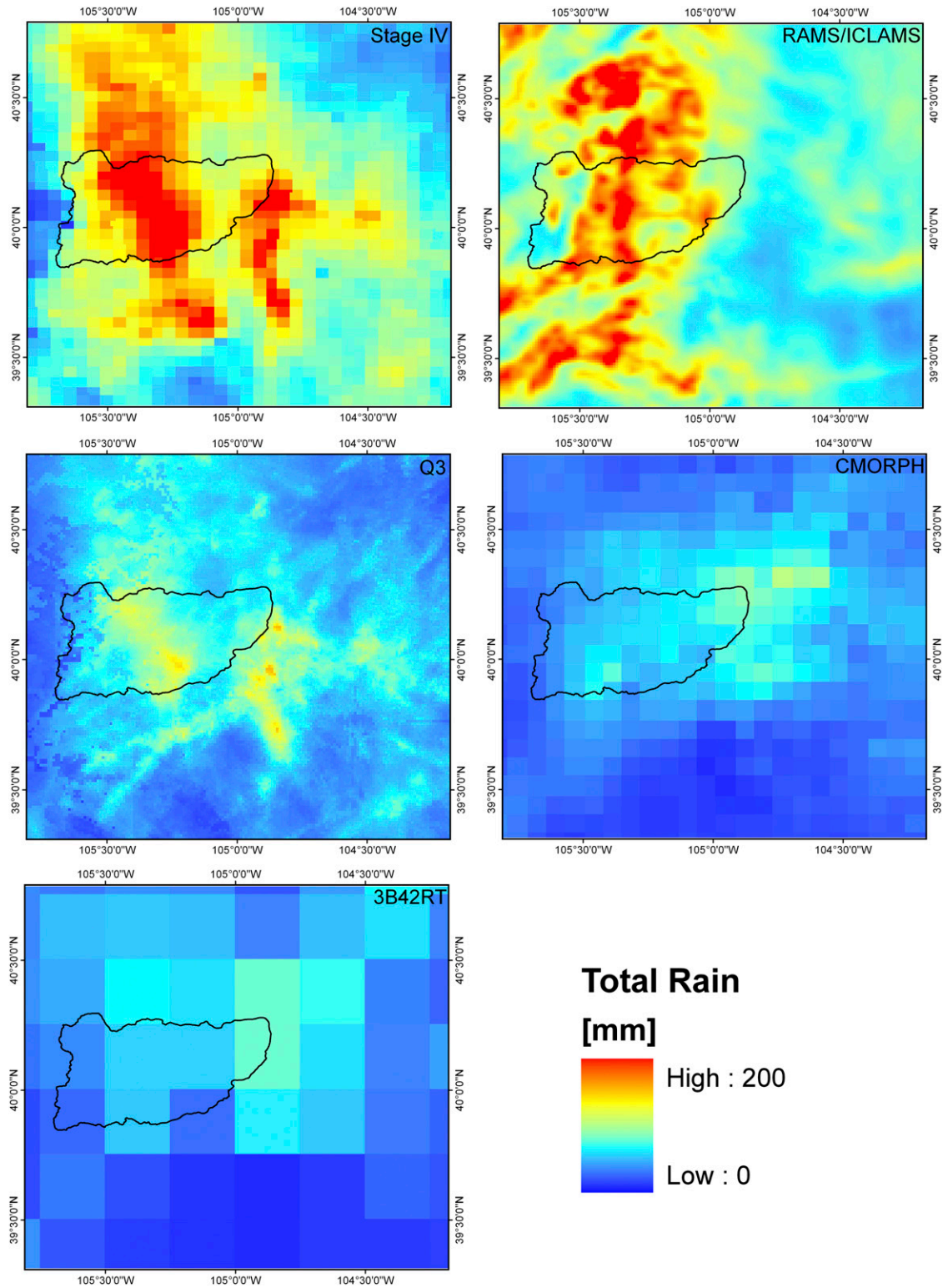


FIG. 2. Rainfall accumulation maps for the various rainfall products involved in the analysis. Note that the accumulation period spans from 0000 UTC 9 Sep to 2300 UTC 13 Sep 2013.

TABLE 2. Storm total rainfall averaged over the whole domain and the basin analyzed for the various rainfall products examined.

Product	Total domain-averaged rainfall (mm)	Total basin-averaged rainfall (mm)
Stage IV	107	158
RAMS-ICLAMS	104	134
MRMS/Q3	55	77
3B42RT	39	50
CMORPH	39	55

entire range of values while there is a nonlinear dependence on rainfall magnitude. This highlights a limitation in adjusting all rainfall values using a single factor (i.e., MFB). The PDF adjustment procedure accounts for magnitude dependence, but its efficiency depends on the accuracy of forecasted rainfall quantiles with respect to the ground truth. The degree of agreement between forecasted and “true” rainfall distribution is manifested in Fig. 3 as the degree of overlap between RAMS-ICLAMS and Stage IV quantiles. Overall, results show that there is good consistency among the two for rainfall intensities $<1.5 \text{ mm h}^{-1}$ (see, e.g., Fig. 3a), which account for $\sim 65\%$ of the hourly rainfall intensity values over the analysis domain, but discrepancies become considerable for higher values where RAMS-ICLAMS consistently underestimates the reference quantiles. The latter indicates that even after PDF adjustment, high RPUE rainfall values will still be underestimated. Moreover, considering that the severe flooding was caused by the high rainfall intensities, it is clear that further improvement is required for forecasting the high rainfall regime.

b. Statistical evaluation of rainfall products

Results from the statistical evaluation of both original and adjusted (indicated by a subscript *adj*) products are summarized in Table 3. Note that the addition of $-MFB_{adj}$ ($-PDF_{adj}$) to the product name denotes the adjusted version of products according to MFB (PDF) adjustment. As shown, MFB adjustment improved bias greatly over the basin, with bias reduction being greater for Q3 and CMORPH and less but still important for 3B42RT. The MFB adjustment is consistently superior to the PDF adjustment when considering the bias ratio. The reason is that PDF adjustment is sensitive to rain detection issues (i.e., missed rain remains zero after PDF adjustment), while the MFB adjustment is not (since it involves only total rainfall ratios). On the other hand, PDF adjustment provides consistently (apart from Q3 over basin) higher improvement in RMSE and correlation coefficient. This was anticipated given that these two metrics reflect the one-to-one correspondence of rainfall (in space or time) between reference and RPUE and therefore would be influenced more by the dynamic adjustment associated with PDF matching.

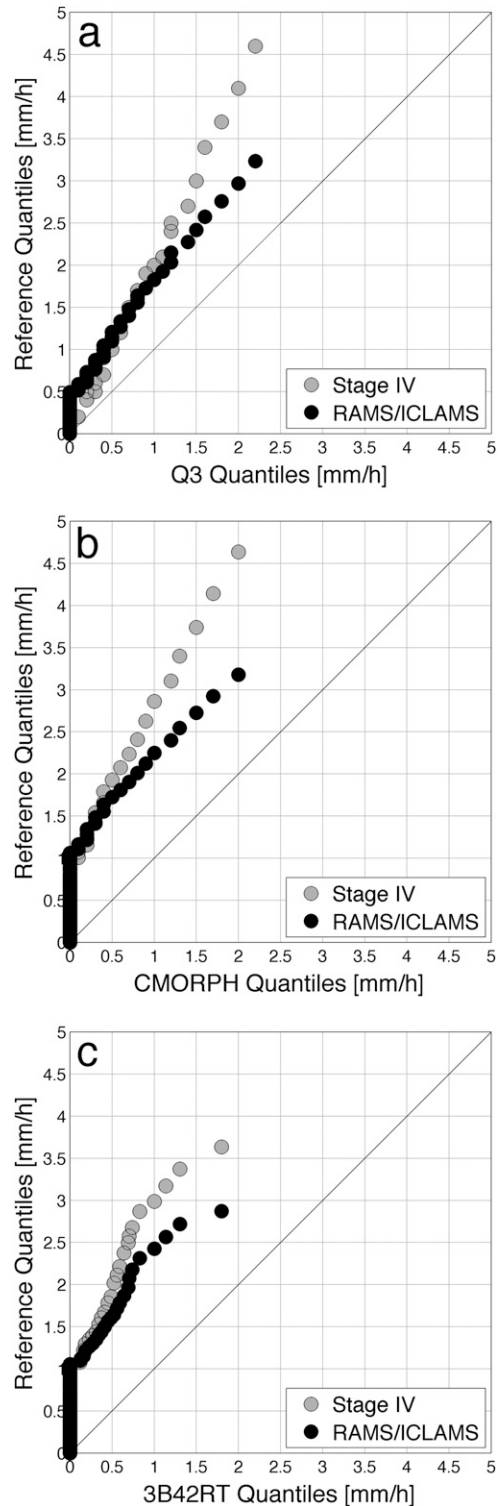


FIG. 3. The $Q-Q$ plots between reference (Stage IV and RAMS-ICLAMS) rainfall and (a) Q3, (b) CMORPH, or (c) 3B42RT. Note that quantiles show the range between the 5th and 95th quantile, with 1% increment.

TABLE 3. Statistical metrics comparing rainfall from Stage IV, with forecasted rainfall from RAMS-ICLAMS and the raw and adjusted Q3, 3B42RT, and CMORPH products. For each metric, the best results among adjustment procedures are indicated in boldface.

Product	Based on domain accumulated rainfall			Based on basin-averaged rainfall		
	Bias ratio	RMSE (mm)	Correlation coef	Bias ratio	RMSE (mm h ⁻¹)	Correlation coef
RAMS-ICLAMS	0.97	48.6	0.36	0.85	2.1	-0.1
Q3	0.51	59.5	0.84	0.48	1.2	0.93
Q3-MFB _{adj}	0.97	1.26	0.84	0.92	0.63	0.93
Q3-PDF _{adj}	0.89	1.1	0.84	0.82	0.78	0.93
3B42RT	0.36	78.2	0.4	0.35	1.7	0.37
3B42RT-MFB _{adj}	0.97	54.5	0.4	0.85	2	0.37
3B42RT-PDF _{adj}	0.79	45.7	0.47	0.7	1.6	0.42
CMORPH	0.37	80.1	0.34	0.32	1.73	0.46
CMORPH-MFB _{adj}	0.97	51.8	0.34	0.92	2.1	0.46
CMORPH-PDF _{adj}	0.75	49.7	0.41	0.7	1.6	0.5

One prominent outcome from the analysis is the particularly poor correlation in basin-averaged time series from forecasted rainfall. To get a better insight into the temporal dynamics of rainfall estimates over the basin, time series for all products (original and adjusted) are presented in Fig. 4. As it is shown, poor correlation of forecasted time series is mainly a result of shifted rainfall patterns. Specifically, forecasted rainfall peaks between 11 and 12 September appear sooner in the series (relative to Stage IV) and are associated with an approximate shift of 12 h. Similar and even greater time shifts in rainfall forecasts for this particular event have also been reported in Hamill (2014). Early triggering of convection by the model is apparently one of the main reasons for the discrepancies between reference and simulated spatial rainfall patterns shown in Fig. 2. Further examination of Fig. 4 reveals that the application of the different adjustment procedures results in instances where rainfall estimates are improved (see results during 12–13 September) or deteriorate (see results for CMORPH and 3B42RT on 10 September). This is an indication that the proposed adjustment procedure cannot account for the temporal variability of bias and PDF differences.

5. Conclusions and future steps

The main objective of this study was to investigate and demonstrate the potential use of NWP forecasts for adjusting remotely sensed (from radar and satellite) rainfall estimates. The 2013 Colorado flood event was chosen as the case study for two particular reasons. First, as it has been shown in this study and others (Gochis et al. 2015), it is an example case for highlighting rainfall underestimation from real-time or near-real-time remote sensing products in a complex-terrain environment. Second, it involves a well-instrumented area, thus allowing independent verification of the proposed NWP-based adjustment procedure. The particular findings of this

work for the case of the 2013 Colorado flood are summarized as follows.

The QPE from all remote sensing products examined (Q3, CMORPH, and 3B42RT) exhibited severe underestimation, reporting only 30%–50% of the reference rainfall (Stage IV). This clearly highlights the issue of QPE underestimation from remote sensing alone during complex-terrain heavy precipitation events.

High-resolution (1 km) forecasts from RAMS-ICLAMS captured the magnitude of total rainfall in the area of analysis well, although shifts in spatial and temporal patterns of rainfall were apparent. Comparison of these results to the work of Lavers and Villarini (2013), who analyzed rainfall forecasts for this event but from a coarser model resolution, confirms that using high-resolution models to forecast rainfall over complex terrain provides a great improvement in forecasted rainfall bias. Overall, model results indicate that considering the overall distribution/amount of forecasted rainfall during the entire event can provide guidance for adjusting the bias in the remotely sensed QPE, although application of the methodology at the subevent scale may be problematic because of temporal shifts. This can be considered a limitation given that significant changes in precipitation structure/type during an event, as reported in Gochis et al. (2015), may be related to considerable changes in the error properties of remote sensing estimates.

Both MFB and PDF adjustment approaches resulted in significant improvement of QPE over all scales examined. MFB provided consistently better bias reduction than PDF adjustment, but the latter improved the RMSE and correlation more. An important note is that after adjustment, RPUE error metrics were better than those obtained from forecasted rainfall. This highlights the benefit of combining NWP with RPUE to obtain QPE over mountainous areas.

Using models to adjust observations can be considered an unorthodox approach. However, evidence from

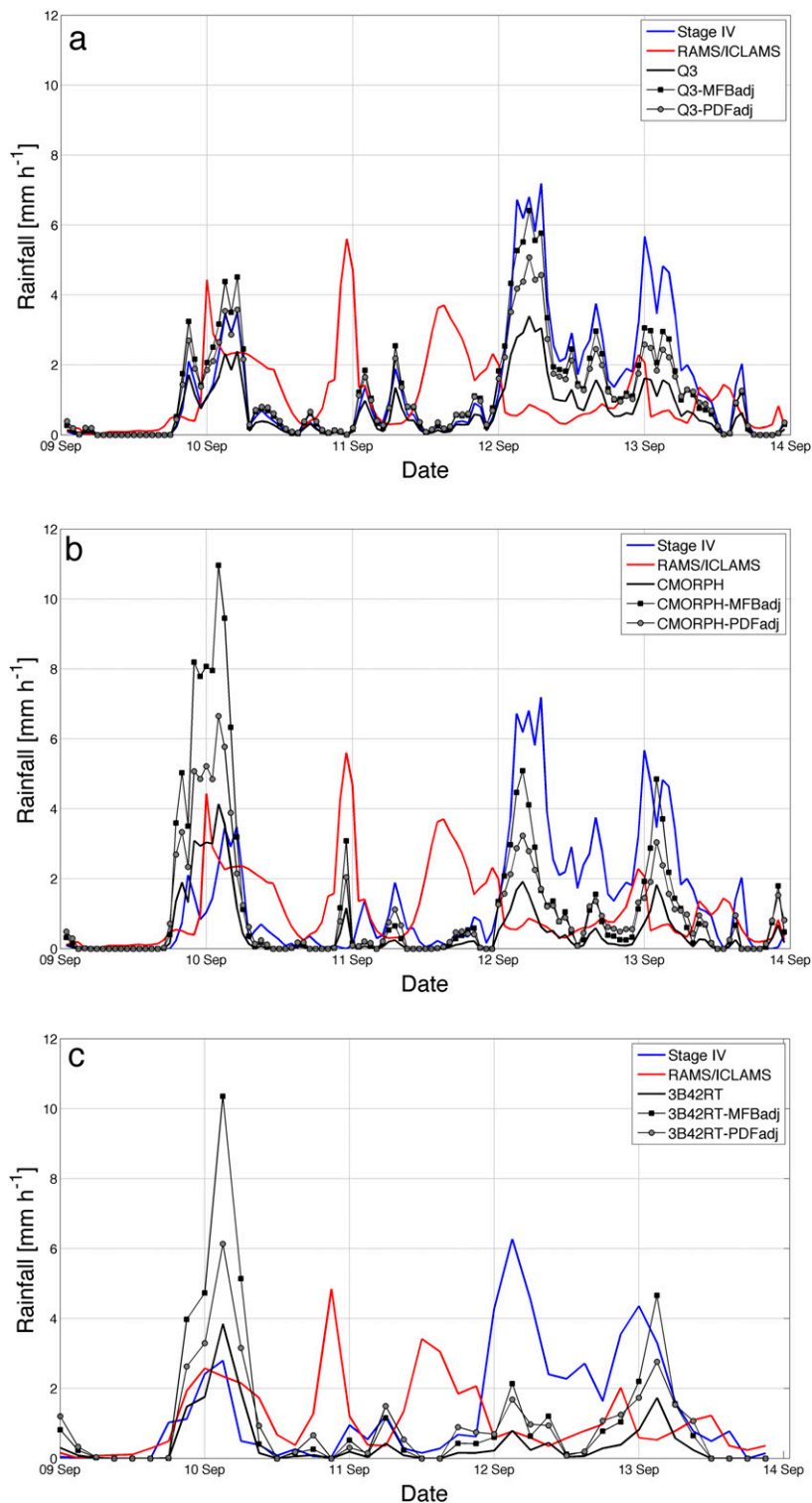


FIG. 4. Time series of basin-averaged rainfall obtained from original and adjusted products of (a) Q3, (b) CMORPH, and (c) 3B42RT. Time series corresponding to Stage IV and RAMS-ICLAMS are also shown for comparison. Note that results for 3B42RT are shown at 3-h time scale.

this and previous work (Zhang et al. 2013) confirms that there is benefit in using high-resolution NWP models for improving remote sensing QPE in the case of heavy precipitation from warm rain events occurring over mountainous terrain. Indisputably, a larger-scale investigation of this concept involving a greater number of events over different regions is needed to arrive to robust conclusions. It is important to note that the work presented does not imply that an NWP-based adjustment should be treated as a replacement of current established techniques. It is clear that the effectiveness of such an approach is heavily dependent on the accuracy of rainfall forecasts and thus should be treated with caution. Especially in the case of real-time applications (e.g., flood forecasting), utilizing this method would imply that rainfall forecasts are used without prior validation—an element that, while offering useful lead time, may also be associated with significant uncertainty. However, for areas with sparse ground observations, such an approach can hold considerable potential for hydrological applications in retrospect (e.g., improve available satellite-rainfall estimates to allow long-term hydrologic analysis). Therefore, future work should focus on evaluating the impact of these NWP-based adjusted products in hydrologic simulations.

Acknowledgments. This work was supported by the EU funded Earth2Observe (ENVE.2013.6.3-3) project and a NASA Precipitation Measurement Mission Award (NNX07AE31G). The authors thank the three anonymous reviewers for providing constructive comments that helped us to improve this work.

REFERENCES

- Barahona, D., and A. Nenes, 2009: Parameterizing the competition between homogeneous and heterogeneous freezing in ice cloud formation—Polydisperse ice nuclei. *Atmos. Chem. Phys.*, **9**, 5933–5948, doi:10.5194/acp-9-5933-2009.
- Boushaki, F. I., K.-L. Hsu, S. Sorooshian, G.-H. Park, S. Mahani, and W. Shi, 2009: Bias adjustment of satellite precipitation estimation using ground-based measurement: A case study evaluation over the southwestern United States. *J. Hydrometeorol.*, **10**, 1231–1242, doi:10.1175/2009JHM1099.1.
- Chumchean, S., A. Sharma, and A. Seed, 2006: An integrated approach to error correction for real-time radar-rainfall estimation. *J. Atmos. Oceanic Technol.*, **23**, 67–79, doi:10.1175/JTECH1832.1.
- Farr, T. G., and Coauthors, 2007: The Shuttle Radar Topography Mission. *Rev. Geophys.*, **45**, RG2004, doi:10.1029/2005RG000183.
- Fountoukis, C., and A. Nenes, 2005: Continued development of a cloud droplet formation parameterization for global climate models. *J. Geophys. Res.*, **110**, D11212, doi:10.1029/2004JD005591.
- Fulton, R. A., J. P. Breidenbach, D.-J. Seo, D. A. Miller, and T. O'Bannon, 1998: The WSR-88D rainfall algorithm. *Wea. Forecasting*, **13**, 377–395, doi:10.1175/1520-0434(1998)013<0377:TWRA>2.0.CO;2.
- Gochis, D., and Coauthors, 2015: The Great Colorado Flood of September 2013. *Bull. Amer. Meteor. Soc.*, doi:10.1175/BAMS-D-13-00241.1, in press.
- Goudenhoofd, E., and L. Delobbe, 2009: Evaluation of radar–gauge merging methods for quantitative precipitation estimates. *Hydrol. Earth Syst. Sci.*, **13**, 195–203, doi:10.5194/hess-13-195-2009.
- Habib, E., A. Henschke, and R. F. Adler, 2009: Evaluation of TMPA satellite-based research and real-time rainfall estimates during six tropical-related heavy rainfall events over Louisiana, USA. *Atmos. Res.*, **94**, 373–388, doi:10.1016/j.atmosres.2009.06.015.
- Hamill, T. M., 2014: Performance of operational model precipitation forecast guidance during the 2013 Colorado front-range floods. *Mon. Wea. Rev.*, **142**, 2609–2618, doi:10.1175/MWR-D-14-00007.1.
- Huffman, G. J., and Coauthors, 2007: The TRMM Multisatellite Precipitation Analysis (TMPA): Quasi-global, multiyear, combined-sensor precipitation estimates at fine scales. *J. Hydrometeorol.*, **8**, 38–55, doi:10.1175/JHM560.1.
- Iacono, M. J., E. J. Mlawer, S. A. Clough, and J.-J. Morcrette, 2000: Impact of an improved longwave radiation model, RRTM, on the energy budget and thermodynamic properties of the NCAR community climate model, CCM3. *J. Geophys. Res.*, **105**, 14 873–14 890, doi:10.1029/2000JD900091.
- Joyce, R. J., J. E. Janowiak, P. A. Arkin, and P. Xie, 2004: CMORPH: A method that produces global precipitation estimates from passive microwave and infrared data at high spatial and temporal resolution. *J. Hydrometeorol.*, **5**, 487–503, doi:10.1175/1525-7541(2004)005<0487:CAMTPG>2.0.CO;2.
- Krajewski, W. F., 1987: Cokriging radar-rainfall and rain gage data. *J. Geophys. Res.*, **92**, 9571–9580, doi:10.1029/JD092iD08p09571.
- Kushita, J., G. Kallos, M. Astitha, S. Solomos, C. Spyrou, C. Mitsakou, and J. Lelieveld, 2014: Impact of natural aerosols on atmospheric radiation and consequent feedbacks with the meteorological and photochemical state of the atmosphere. *J. Geophys. Res. Atmos.*, **119**, 1463–1491, doi:10.1002/2013JD020714.
- Lavers, D. A., and G. Villarini, 2013: Were global numerical weather prediction systems capable of forecasting the extreme Colorado rainfall of 9–16 September 2013? *Geophys. Res. Lett.*, **40**, 6405–6410, doi:10.1002/2013GL058282.
- Lin, Y., and K. E. Mitchell, 2005: The NCEP Stage II/IV hourly precipitation analyses: Development and applications. Preprints, *19th Conf. on Hydrology*, San Diego, CA, Amer. Meteor. Soc., 1.2. [Available online at <http://ams.confex.com/ams/pdfpapers/83847.pdf>.]
- Meyers, M. P., R. L. Walko, J. Y. Harrington, and W. R. Cotton, 1997: New RAMS cloud microphysics parameterization. Part II: The two-moment scheme. *Atmos. Res.*, **45**, 3–39, doi:10.1016/S0169-8095(97)00018-5.
- Mlawer, E. J., S. J. Taubman, P. D. Brown, M. J. Iacono, and S. A. Clough, 1997: Radiative transfer for inhomogeneous atmospheres: RRTM, a validated correlated-*k* model for the longwave. *J. Geophys. Res.*, **102**, 16 663–16 682, doi:10.1029/97JD00237.
- Müller, M. F., and S. E. Thompson, 2013: Bias adjustment of satellite rainfall data through stochastic modeling: Methods development and application to Nepal. *Adv. Water Resour.*, **60**, 121–134, doi:10.1016/j.advwatres.2013.08.004.
- Nikolopoulos, E. I., E. N. Anagnostou, and M. Borga, 2013: Using high-resolution satellite rainfall products to simulate a major flash flood event in northern Italy. *J. Hydrometeorol.*, **14**, 171–185, doi:10.1175/JHM-D-12-09.1.
- Seo, D.-J., and J. P. Breidenbach, 2002: Real-time correction of spatially nonuniform bias in radar rainfall data using rain gauge measurements. *J. Hydrometeorol.*, **3**, 93–111, doi:10.1175/1525-7541(2002)003<0093:RTCOSN>2.0.CO;2.

- Smith, J. A., M. L. Baeck, M. Steiner, and A. J. Miller, 1996: Catastrophic rainfall from an upslope thunderstorm in the central Appalachians: The Rapidan storm of June 27, 1995. *Water Resour. Res.*, **32**, 3099–3113, doi:[10.1029/96WR02107](https://doi.org/10.1029/96WR02107).
- Solomos, S., G. Kallos, J. Kushta, M. Astitha, C. Tremback, A. Nenes, and Z. Levin, 2011: An integrated modeling study on the effects of mineral dust and sea salt particles on clouds and precipitation. *Atmos. Chem. Phys.*, **11**, 873–892, doi:[10.5194/acp-11-873-2011](https://doi.org/10.5194/acp-11-873-2011).
- Stampoulis, D., E. N. Anagnostou, and E. I. Nikolopoulos, 2013: Assessment of high-resolution satellite-based rainfall estimates over the Mediterranean during heavy precipitation events. *J. Hydrometeor.*, **14**, 1500–1514, doi:[10.1175/JHM-D-12-0167.1](https://doi.org/10.1175/JHM-D-12-0167.1).
- Tesfagiorgis, K., S. E. Mahani, N. Y. Krakauer, and R. Khanbilvardi, 2011: Bias correction of satellite rainfall estimates using a radar-gauge product—A case study in Oklahoma (USA). *Hydrol. Earth Syst. Sci.*, **15**, 2631–2647, doi:[10.5194/hess-15-2631-2011](https://doi.org/10.5194/hess-15-2631-2011).
- Wang, G., L. Liu, and Y. Ding, 2012: Improvement of radar quantitative precipitation estimation based on real-time adjustments to Z - R relationships and inverse distance weighting correction schemes. *Adv. Atmos. Sci.*, **29**, 575–584, doi:[10.1007/s00376-011-1139-8](https://doi.org/10.1007/s00376-011-1139-8).
- Wilson, J. W., and D. M. Pollock, 1974: Rainfall measurements during Hurricane Agnes by three overlapping radars. *J. Appl. Meteor.*, **13**, 835–844, doi:[10.1175/1520-0450\(1974\)013<0835:RMDHAB>2.0.CO;2](https://doi.org/10.1175/1520-0450(1974)013<0835:RMDHAB>2.0.CO;2).
- Yin, Z.-Y., X. Zhang, X. Liu, M. Colella, and X. Chen, 2008: An assessment of the biases of satellite rainfall estimates over the Tibetan Plateau and correction methods based on topographic analysis. *J. Hydrometeor.*, **9**, 301–326, doi:[10.1175/2007JHM903.1](https://doi.org/10.1175/2007JHM903.1).
- Zhang, J., and Coauthors, 2011: National Mosaic and Multi-Sensor QPE (NMQ) system: Description, results, and future plans. *Bull. Amer. Meteor. Soc.*, **92**, 1321–1338, doi:[10.1175/2011BAMS-D-11-00047.1](https://doi.org/10.1175/2011BAMS-D-11-00047.1).
- Zhang, X., E. N. Anagnostou, M. Frediani, S. Solomos, and G. Kallos, 2013: Using NWP simulations in satellite rainfall estimation of heavy precipitation events over mountainous areas. *J. Hydrometeor.*, **14**, 1844–1858, doi:[10.1175/JHM-D-12-0174.1](https://doi.org/10.1175/JHM-D-12-0174.1).